EXTENDING MEAN-FIELD THEORIES OF STRUCTURE FORMATION IN INCOMPRESSIBLE MAGNETOHYDRODYNAMIC TURBULENCE

Suying Jin
Department of Astrophysical Sciences,
Princeton University
Princeton Plasma Physics Laboratory
Princeton, NJ 08540 USA
sjin@pppl.gov

Ilya Y. Dodin
Princeton Plasma Physics Laboratory
Department of Astrophysical Sciences,
Princeton University
Princeton, NJ 08540 USA
idodin@pppl.gov

ABSTRACT

Structure formation in magnetohydrodynamic (MHD) turbulence can be modeled as a modulational instability (MI) of the fluctuations comprising the background turbulence. We focus on the early stages of structure formation and consider simple backgrounds in order to develop a tractable model. Unlike typical calculations of MI, we retain not only the first but all modulational harmonics. This allows us to examine the validity of the popular quasilinear (QL) closure which truncates the modulational spectrum after the first harmonic. For ideal incompressible MHD, we find that the QL closure can be quantitatively accurate in some regimes; yet, in adjacent regimes it fails to predict the modulational dynamics even qualitatively, predicting MIs when the system is, in fact, modulationally stable. In those regimes, the dynamics is dominated by propagating spectral waves (PSWs), which ballistically transport energy along the spectrum. This effectively introduces dissipation to ideal MHD, thereby reducing the instability rate or eliminating MI entirely. PSWs correspond to modulational eigenmodes with flat energy spectra (up to dissipative scales), so the total modulational energy grows linearly in time as the energy front propagates down the spectrum at the group velocity of the PSW. That said, this picture is specific to ideal MHD, and adding corrections to the governing equations (e.g. dissipation, dispersive effects) tends to suppress PSWs and reinstate the validity of the QL closure.

INTRODUCTION

Coherent-structure formation from turbulence is ubiquitous in nature, intrinsically compelling, and one of the precious few aspects of turbulence that are relatively yielding to analytical efforts (Hussain, 1986; Smolyakov *et al.*, 2000; Krashennikov *et al.*, 2008). For magnetohydrodynamic (MHD) turbulence (Biskamp, 2003; Beresnyak, 2019; Schekochihin, 2022) and the turbulent-dynamo problem (Brandenburg *et al.*, 2012; Tobias, 2021; Rincon *et al.*, 2016), this has spawned a vast body of work known as mean-field electrodynamics (Rädler, 2007; Moffatt, 1978; Brandenburg, 2018). In such approaches, the velocity and magnetic fields are split into fluctuations and mean fields; then, various closures are implemented to obtain the mean-field evolution in response to the fluctuations (Blackman & Field, 2002; Kraichnan, 1977; Nicklaus & Stix, 1988).

In this paper, we are concerned with the popular quasilinear approximation (QLA) (also known as the first-order smoothing (Krause & Rädler, 1980) or second-order correlation approximation (Rädler, 1982)), which assumes that the mean-field evolution is determined only by second-order correlations of the fluctuations (Dodin, 2022). Despite its limited regime of formal validity, the QLA endures in its popularity as a workhorse that is too convenient to cast aside in analytical calculations (Squire & Bhattacharjee, 2015; Masada & Sano, 2014; Gopalakrishnan & Singh, 2023). Furthermore, in some cases, QL calculations have been found to produce good agreement with direct numerical simulations (DNS) even outside of their formal validity domain (Käpylä *et al.*, 2006). It is therefore important to understand when, and how exactly, the QLA fails. Answering this question requires exploring a mean-field model that retains high-order correlations.

Here, we explore structure formation in MHD turbulence as a modulational instability (Zakharov & Ostrovsky, 2009) (MI) of the flow-velocity and magnetic-field fluctuations comprising the background turbulence, using an 'extended' quasilinear theory (XQL) that treats the primary structure as fixed but includes the entire spectrum of modulational harmonics, i.e. the high-order correlations. Due to size limitations, only the main results will be presented, but further details can be found in an extended version of this paper (Jin & Dodin, 2024).

MODEL
Base Model: 2-D Ideal Incompressible MHD

As a base model, we assume ideal incompressible MHD with homogeneous mass density $\rho = $ const. The correspond-

ing governing equations written in the Elsässer variables, $z^\pm \doteq v \pm b$, are

$$\partial_t z^\pm = -(z^\mp \cdot \nabla)z^\pm - \nabla p. \tag{1}$$

Here v is the fluid velocity; $b \doteq B/\sqrt{4\pi\rho}$ is the magnetic field B in units of the local Alfvén velocity; and $p \doteq (P + B^2/8\pi)/\rho$ is the normalized total pressure, with P being the kinetic pressure. Due to incompressibility and magnetic Gauss's law, one also has $\nabla \cdot z^\pm = 0$. Although we do not explicitly include the viscosity and resistivity, they are tacitly retained in our discussion of spectral propagation and its associated anomalous dissipation.

We also adopt a two-dimensional (2-D) model in which $z^\pm$ lie in the (x, y) plane and $\partial_z = 0$, such that we need only keep track of the z-component of the Elsässer vorticities, $w^\pm \doteq [\nabla \times z^\pm]_z = \partial_x z_y^\pm - \partial_y z_x^\pm$. Then, (1) can be replaced with a scalar equation for $w^\pm$, which leads to the following equations for the Fourier coefficients $w_k^\pm(t)$:

$$\partial_t w_k^\pm = \sum_{k_1, k_2} T(k_1, k_2) w_{k_1}^\mp w_{k_2}^\pm \delta_{k, k_2 + k_1}, \tag{2}$$

where $T(k_1, k_2) \doteq \frac{[e_z \cdot (k_2 \times k_1)]}{k_1^2 k_2^2}(k_2 + k_1) \cdot k_2$ are the coupling coefficients, and δ is the Kronecker delta.

Although the dynamo effect is not possible in 2-D (an anti-dynamo theorem by Zeldovich (1957)), (2) hosts a rich variety of modulational dynamics in which energy can be transferred between primary fluctuations and mean structures, and between velocity and magnetic fields, as shown in figure 1. (The corresponding notation is introduced below.)

Coupling Dominated by a Primary Structure.

Let us explore modulational stability of a spatial structure with a given wavevector $k = p$ to a perturbation with a wavevector q, where $p \cdot q = 0$. Let us also assume $w_p^\pm = \mathcal{O}(1)$, $w_{q+np}^\pm = \mathcal{O}(\varepsilon)$, and same for any other $w_{k \neq p}^\pm$, where $\varepsilon \ll 1$ is a small parameter. Then, by linearizing (2) in ε, one obtains the following chain of equations:

$$\partial_t w_k^\pm \approx T(p, k_-)w_p^\mp w_{k_-}^\pm + T(-p, k_+)w_{-p}^\mp w_{k_+}^\pm$$
$$+ T(k_-, p)w_{k_-}^\mp w_p^\pm + T(k_+, -p)w_{k_+}^\mp w_{-p}^\pm, \tag{3}$$

where $k_\pm \doteq k \pm p$ and $k = q + np$ with integer n. For all other k, one obtains $\partial_t w_k^\pm \approx 0$. In particular, this means that $w_p^\pm$ can be considered fixed; i.e. $A^\pm \doteq w_p^\pm \approx \text{const}$. In terms of the Elsässer fields, this corresponds to a primary structure

$$z^\pm = -\frac{2}{p}\mathcal{A}^\pm \sin(py + \theta^\pm)e_x, \tag{4}$$

where $\mathcal{A}^\pm \doteq |A^\pm|$ and $\theta^\pm \doteq \arg A^\pm$.

The modulational and primary energy densities are respectively:

$$E_{\text{mod}} \doteq \sum_{k=q+np} E_k = \sum_n \frac{\rho}{4} \frac{|w_{q+np}^+|^2 + |w_{q+np}^-|^2}{q^2 + n^2 p^2}, \tag{5a}$$

$$E_{\text{pri}} \doteq E_p = \frac{\rho}{4} \frac{|w_p^+|^2 + |w_p^-|^2}{p^2}, \tag{5b}$$

where 'c.c.' stands for 'complex conjugate'.

Our approximate equations conserve the total energy density $E_{\text{tot}} = E_{\text{pri}} + E_{\text{mod}}$ exactly within the approximation. (For brevity, from now on we will refer to the energy densities simply as energies.) We will assume that the initial modulational energy is negligible, so $E_{\text{tot}} = \rho\mathcal{A}^2/4p^2$, where $\mathcal{A}^2 \doteq (\mathcal{A}^+)^2 + (\mathcal{A}^-)^2$.

Extended quasilinear theory. In order to reduce the number of free parameters, let us take $\mathcal{A}^+ = \mathcal{A}^-$ (a more general version can be found in Jin & Dodin (2024)), introduce the dimensionless time, $\tau \doteq \mathcal{A}t$, and perform a variable transformation $w_{q+np}^\pm \mapsto y_n^\pm$: $w_{q+np}^\pm = \mathcal{A}\sqrt{(q^2/p^2 + n^2)}\exp\left(in\frac{\theta^+ + \theta^-}{2}\right)y_n^\pm$.

Then, (3) becomes

$$\dot{y}_n = G_n^- y_{n-1} + G_n^+ y_{n+1}, \tag{6a}$$

$$G_n^\pm \doteq \frac{1}{\sqrt{2}}\begin{pmatrix} \alpha_n^\pm e^{\mp i\theta} & \beta_n^\pm e^{\pm i\theta} \\ \beta_n^\pm e^{\mp i\theta} & \alpha_n^\pm e^{\pm i\theta} \end{pmatrix}, \tag{6b}$$

$$\alpha_n^\pm \doteq \mp r\frac{r^2 + n(n \pm 1)}{\sqrt{(r^2 + n^2)(r^2 + (n \pm 1)^2)}}, \tag{6c}$$

$$\beta_n^\pm \doteq -r\frac{n}{\sqrt{(r^2 + n^2)(r^2 + (n \pm 1)^2)}}, \tag{6d}$$

where the dot denotes ∂_τ, and $y_n \doteq (y_n^-, y_n^+)^\mathsf{T}$ is a two-component column vector (the symbol T denotes transposition). The parameter $r \doteq q/p$ represents the relative scales of the modulation and primary structure, while $\theta \doteq (\theta^+ - \theta^-)/2$ determines the relative weights of the kinetic and magnetic-field energy in the primary-mode ($|b_p|^2/|v_p|^2 = \tan^2\theta$.) At $\theta < \pi/2$, one has a velocity-dominated primary mode (VDPM); that is, the kinetic energy of the primary mode is larger than the corresponding magnetic energy, and vice versa at $\theta > \pi/2$ (BDPMs). The parameters r, and θ entirely determine the dynamics of (6), while $\mathcal{A}$ and p determine only its characteristic temporal and spatial scales, respectively.

Throughout this work, we use (6) and (13a) to study the nature of collective oscillations in the chain of modulational harmonics, which can be understood as Floquet modes of the linearised system. The nth elementary cell of the chain consists of two coupled oscillators characterised by y_n^+ and y_n^-, respectively. Unstable global modes of this system (i.e. MIs) lead to structure formation on top of the primary structure.

To emulate a simple modulation, in DNS of (6), we will use initial conditions of the form:

$$y_n^\pm(\tau = 0) = \begin{cases} \varepsilon \exp(i\xi_n^\pm), & n = \pm 1, \\ 0, & n \neq \pm 1. \end{cases} \tag{7}$$

Here, ε is a constant small amplitude, and ξ_n are parameters that change the polarization of the initial conditions while keeping the initial energy fixed. (The specific values of $\xi_n^\pm$ are given in the captions of figures showing results of DNS.)

Energy equations. At second order in ε, one obtains the following equations for the energy densities:

$$\mathcal{E}_{\text{mod}} \doteq \frac{E_{\text{mod}}}{E_{\text{tot}}} = \sum_n |y_n^+|^2 + |y_n^-|^2 \equiv \sum_n \mathcal{E}_n, \tag{8}$$

$$\dot{\mathcal{E}}_n = (I_n^+ + F_n^+) + (I_n^- + F_n^-) + \text{c.c.}, \tag{9}$$

Figure 1. DNS of modulational dynamics of (1) seeded at $\tau = 0$ with random noise. Figures (a), (c), and (e) correspond to a modulationally unstable primary mode (4) with $\theta^\pm = \pm\pi/6$, and (b), (d), and (f) correspond to a modulationally stable primary mode with $\theta^\pm = \pm\pi/3$. Figures (a) and (b) show $z_x^+(t,y)$, (c) and (d) show $z_y^+(t,x)$, and (e) and (f) show the corresponding energy breakdown. Specifically, $\mathcal{E}_v = E_v/E_{\mathrm{tot}}$ is the normalised kinetic energy, $\mathcal{E}_b = E_b/E_{\mathrm{tot}}$ is the normalised magnetic energy, $\mathcal{E}_{\mathrm{mod}}$ is the normalised modulational-mode energy (9), and $\mathcal{E}_{\mathrm{pri}}$ is the normalised primary-mode energy (10). The colour bar shows the field amplitudes normalised to $\mathcal{A}/p$. The spatial coordinates are normalised to $1/p$.

$$\dot{\mathcal{E}}_{\mathrm{pri}} \doteq \frac{\dot{E}_{\mathrm{pri}}}{E_{\mathrm{tot}}} = -\sum_n I_n^+ + I_n^- + \mathrm{c.c.}, \qquad (10)$$

where $I_n^\pm$ and $F_n^\pm$ are given by

$$I_n^\pm = (\beta_n^- \mathrm{e}^{\pm\mathrm{i}\theta} y_{n-1}^\mp + \beta_n^+ \mathrm{e}^{\mp\mathrm{i}\theta} y_{n+1}^\mp) y_n^{\pm*}, \qquad (11)$$

$$F_n^\pm = (\alpha_n^- \mathrm{e}^{\mp\mathrm{i}\theta} y_{n-1}^\pm + \alpha_n^+ \mathrm{e}^{\pm\mathrm{i}\theta} y_{n+1}^\pm) y_n^{\pm*}. \qquad (12)$$

The terms $F_n^\pm$ represent the energy flux that is carried along the modulation spectrum and is conserved within each sub-channel, $y^\pm$ ($\sum_n F_n^\pm = 0$). In contrast, the $I_n^\pm$ terms can be understood as energy exchange between the modulational and primary modes in that they appear in both (10) and (9) with opposite signs. The important features to note in (11) is that the energy injection into harmonic n is proportional both to the approximate local energy density, as well as a coupling coefficient, $|\beta_n^\pm| \sim 1/|n|$. The former implies that injection can form positive feedback loops to drive MIs, while the latter enforces that such injection is localized at small n.

Relationship to quasilinear approximation.
The QLA amounts to a truncation of (6) at the first harmonic (i.e. setting all $y_{|n|>1} = 0$). We will see that the modulational dynamics of the truncated system can be qualitatively different from those predicted by nonlinear MHD (1) and XQL (6). The latter two are in agreement as long as the underlying ordering assumption ($|w_{q+np}^\pm|/|w_p^\pm| \sim \mathcal{O}(\varepsilon)$) holds, i.e. XQL and its fully nonlinear base model have identical linear properties such as growth rates. In the remainder of this work, we discuss to what extent such truncations can be adequate and compare our analytical results to DNS of (6), in lieu of (1).

RESULTS
Modulational Instabilities

Equation (6) can be written as a vector equation

$$\dot{\boldsymbol{y}} = \boldsymbol{M}\boldsymbol{y}, \qquad (13\mathrm{a})$$

$$\boldsymbol{M} \doteq \begin{pmatrix} \ddots & & \vdots & & \cdot{\cdot} \\ & 0 & \boldsymbol{G}_{-2}^+ & 0 & 0 & 0 \\ & \boldsymbol{G}_{-1}^- & 0 & \boldsymbol{G}_{-1}^+ & 0 & 0 \\ \cdots & 0 & \boldsymbol{G}_0^- & 0 & \boldsymbol{G}_0^+ & 0 & \cdots \\ & 0 & 0 & \boldsymbol{G}_1^- & 0 & \boldsymbol{G}_1^+ \\ & 0 & 0 & 0 & \boldsymbol{G}_2^- & 0 \\ \cdot{\cdot} & & \vdots & & \ddots \end{pmatrix}, \qquad (13\mathrm{b})$$

where $\boldsymbol{y} \doteq (\ldots, \boldsymbol{y}_{-1}, \boldsymbol{y}_0, \boldsymbol{y}_1 \ldots)^\mathsf{T}$ is an infinite-dimensional block vector consisting of $\boldsymbol{y}_n$, and $\boldsymbol{M}$ is an infinite-dimensional block matrix. The modulational modes of the linearized system are solutions of (13a) of the form $\boldsymbol{y} = \boldsymbol{Y} \exp(-\mathrm{i}\omega t)$ with constant polarization vectors $\boldsymbol{Y}$ and frequencies ω. Correspondingly, MIs are modes with $\mathrm{Im}\,\omega > 0$.

One can also consider (13a) as a Schrödinger equation with a Hamiltonian $\mathrm{i}\boldsymbol{M}$. This Hamiltonian is not Hermitian, because modulations are parametrically coupled with the primary mode (through which energy can be either gained or lost) and dissipate at $n \to \infty$. At the same time, this Hamiltonian is invariant under the time-reversal transformation ($\mathrm{i} \to -\mathrm{i}$) and the parity transformation in the spectral space ($n \to -n$, $\theta \to -\theta$). This makes the system (6) $\mathcal{PT}$-symmetric (Bender, 2005). Depending on the balance of sources and sinks, such systems can support modes with entirely real frequencies (unbroken $\mathcal{PT}$ symmetry) and pairs of modes whose frequencies are mutually complex-conjugate (broken $\mathcal{PT}$ symmetry). This will be discussed further the section on spectral waves.

The QLA yields a truncated system that can be analyti-

3

Figure 2. (a) The growth rate Γ (of the most unstable mode) versus the normalised wavenumber r at $\theta = 0$ as found by QL (blue) and XQL (6) (black markers). (b) Same as (a) for Γ versus θ at $r = 0.5$. (c) Mode structures of MIs supported by VDPMs, $|Y_n|$ versus n, at $r = 0.5$ for various θ. (d) Same as (c) for oscillatory modes supported by BDPMs. (The upper index in $|Y_n^\pm|$ is omitted because $|Y_n^+| = |Y_n^-|$.) The asymptotes are indicated by the dotted lines. These results are obtained through DNS of (6) and normalised such that $|Y_0| = 1$.

cally solved, yielding the following dispersion relation:

$$\omega^2 = \frac{r^2}{1+r^2}\left(r^2 \pm |\cos 2\theta|\right), \tag{14}$$

where the unstable mode corresponds to the $-$ sign. At $\theta = 0$, this reduces to the familiar Kelvin–Helmholtz instability, so (14) can be identified as its MHD generalization. Figures 2(a-b) compare (14) to the growth rates obtained via DNS of the XQL system (6). It can be seen that although the QLA provides good approximations of the MI growth rates for VDPMs, it systematically produces false positives for instability for BDPMs. In particular, it predicts a symmetric (in θ) set of instabilities for BDPMs, while DNS of XQL reveals stable (real ω) modes. XQL also reveals that the underlying mode structures are fundamentally different in the two cases–MIs correspond to modulational eigenmodes that fall off exponentially in $|n|$ while the stable modes supported by BDPMs have flat mode structures, as shown in figures 2(c-d). The dynamics driving these oscillatory modes, and their relationship to stability are the focus of the following sections.

Spectral Waves
Asymptotic form. At $|n| \to \infty$, the coupling coefficients have the following limits: $\alpha_n^\pm \to \mp q/p$ and $\beta_n^\pm \to 0$. Then, (6) reduces to a set of decoupled propagation equations:

$$\dot{y}_n^\pm = \frac{r}{\sqrt{2}}\left(e^{\mp i\theta}y_{n-1}^\pm - e^{\pm i\theta}y_{n+1}^\pm\right). \tag{15}$$

Equation (15) has solutions of the form $y_n^\pm = Y^\pm \exp(-i\omega\tau + iK^\pm n)$, where $Y^\pm = $ const. The spectral wavenumber $K^\pm$ is defined within the Brillouin zone $K \in (-\pi, \pi)$, and ω satisfies

$$\omega = \sqrt{2}r\sin\kappa^\pm, \qquad \kappa^\pm \doteq K^\pm \pm \theta. \tag{16}$$
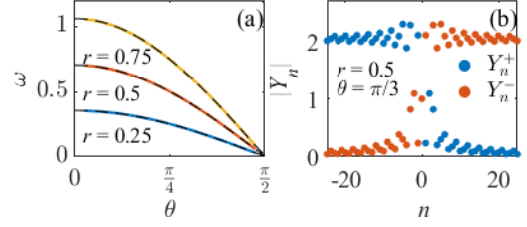
Figure 3. (a) The dependence of the global-mode frequency $\omega > 0$ on θ for various r. The dashed lines are the inferred solutions (17). (b) $|Y_n^+|$ (blue) and $|Y_n^-|$ (orange) for the mode with $\omega > 0$. The eigenmode amplitudes for the $\omega < 0$ mode are identical with the roles of $|Y_n^+|$ and $|Y_n^-|$ switched.

These solutions are understood as *propagating spectral waves* (PSWs), which carry energy along the spectrum (in the $y_n^\pm$ channel) at the spectral group velocity, $v_g^\pm = \sqrt{2}r\cos\kappa^\pm$.

Global modulational modes. In principle, spectral waves with any $K^\pm$ (modulo the Brillouin zone) can exist at large $|n|$, for a given modulational system parametrized by r and θ. However, there are also special PSWs with frequency ω that correspond to that of a global modulational mode (eigenmodes of (13a)), which we find through DNS of (6) to be

$$\omega = \pm\sqrt{2}r\cos\theta. \tag{17}$$

These resonant PSWs are self-sustained as the asymptotic tails of the flat ($|Y_n| \sim$ const.) BDPM eigenmodes shown in figure 2(d). The global mode frequencies and the corresponding detailed mode structure are shown in figure 3.

As these modes are formally of infinite energy (due to their flat energy profile and unbounded extent within (6)), they can never be fully realized. In practice, they will be cut off in n by dissipative scales, or in time by depletion of the primary mode. This process is the focus of the following section.

Effective dissipation and stability. Since a PSW mode carries energy towards $|n| \to \infty$, eventually, a large enough $|n|$ is reached where the energy is dissipated regardless of how small the viscosity and resistivity are. Thus, a PSW exhibits an effective, or 'anomalous', dissipation rate γ that is independent of ν and η in the limit $\nu, \eta \to 0$. This effect is different from the anomalous dissipation caused by eddy–eddy collisions in turbulence (for example, see Donzis *et al.* (2005)) in that the energy transport caused by a PSW is ballistic.

As shown in figure 3(b), a global PSW at large $|n|$ has a flat mode structure, i.e. a structure with $\mathcal{E}_n$ independent of n (see (9)). This structure establishes itself as an expanding 'shelf' whose edges (wave fronts) propagate across the spectrum to $n \to \pm\infty$ at the group velocity v_g. Since the height of the shelf, $\overline{\mathcal{E}_n}$, remains constant, this process drains energy from the primary mode linearly in time, as shown in figure 4.

Figure 5 shows the corresponding anomalous dissipation rate normalised to the seed energy, along with its determining factors – the system-dependent PSW group velocity v_g and the average spectral energy density $\overline{\mathcal{E}_n}$, which is determined by the initial conditions. It can be seen that, for the MI unstable VDPMs ($\theta < \pi/4$), spectral waves are relatively slow and have a small amplitude. The transition to modulational stability occurs at $|v_g| \sim \Gamma$. This condition can be understood as a
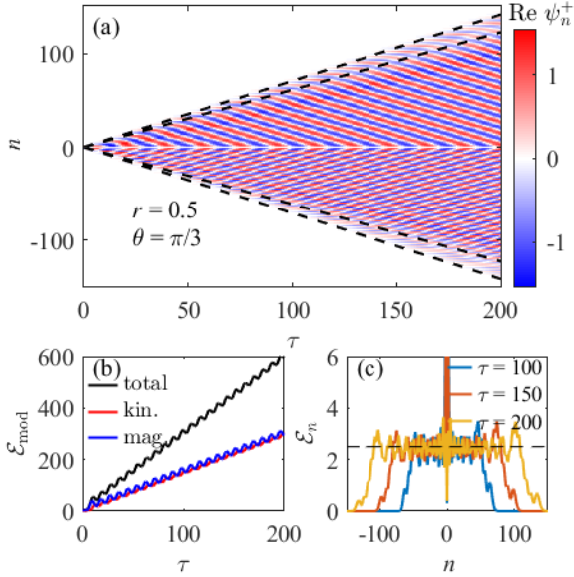
Figure 4. DNS of (6) showing global-mode PSWs for $r = 0.5$, $\theta = \pi/3$: (a) $\mathrm{Re}\,y_n^+/\varepsilon$ for a PSW seeded by the initial conditions (7) with $\xi_d^{\pm} = d\exp(\pm i\pi/4)$ (colour bar). The dashed lines indicate the fronts propagating at: (i) the maximum spectral speed $\sqrt{2}r$ and (ii) the group velocity of the mode. The field between these dashed lines consists of transients. (b) The total energy of the modulation, $\mathcal{E}_{\mathrm{mod}}$, versus τ (black), along with its kinetic (red) and magnetic (blue) components. (c) The profiles of the spectral energy density at $\tau = 100, 150, 200$. The horizontal dashed line indicates the average spectral energy density $\overline{\mathcal{E}_n}$, where the average is taken over the PSW period and over n between the energy fronts.

threshold beyond which (i.e. at $|v_g| \gtrsim \Gamma$) PSWs provide a sufficiently fast escape route for the energy injected at small $|n|$, such that the positive feedback loops (see (11)) supporting MIs can no longer be sustained. In the context of $\mathcal{PT}$ symmetry, the spectral group velocity can be understood as the effective coupling between the links in the oscillator chain, connecting the energy injection from the primary mode at small n to the energy sink at $n \to \infty$. As $|v_g|$ increases with θ, the system transitions from broken to unbroken $\mathcal{PT}$ symmetry.

Modulational Modes Beyond Ideal MHD

As discussed in the previous sections, the existence of PSWs undermines the standard QLA in application to ideal incompressible MHD. Given the ubiquity of QL modeling in the literature, it may seem concerning that the QLA can fail so spectacularly. Interestingly, though, the QLA is somewhat more robust beyond the ideal-MHD limit, both due to conservative corrections and dissipation.

Let us discuss the former first. Without attempting to describe any particular physical system, let us consider the following modified version of (1):

$$\partial_t z^{\pm} = -(z^{\mp} \cdot \nabla)z^{\pm} - \nabla P + \lambda\,\partial_x \nabla^2 z^{\pm}, \qquad (18)$$

where λ is a constant parameter. The last term is intended as a simple ad hoc correction that, while causing deviation from ideal MHD, leaves the primary-mode evolution unaffected and preserves MHD's key invariants, specifically, the energy and
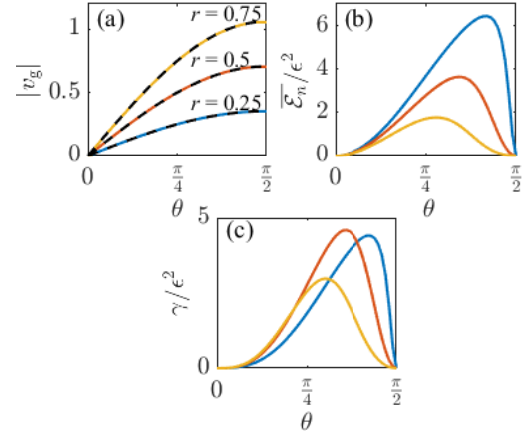
Figure 5. (a) The magnitude of the global PSW group velocity $|v_g|$ versus θ for various r. (b) Same for the average spectral energy density $\overline{\mathcal{E}_n}/\varepsilon^2$. (c) Same for the resulting average drain rate γ/ε^2, where $\gamma \doteq -\dot{\mathcal{E}}_{\mathrm{pri}}/\mathcal{E}_{\mathrm{pri}} = 2|v_g|\overline{\mathcal{E}_n}/\mathcal{E}_{\mathrm{pri}}$. The initial conditions used are given by (7), with $\xi_1^{\pm} = -\xi_{-1}^{\pm} = \exp(\pm i\pi/2)$ which maximizes $\overline{\mathcal{E}_n}$ for all θ.

cross helicity. Similar terms can appear due to a background magnetic field or differential rotation (Heinonen *et al.*, 2023).

With this correction, one arrives at the following corresponding modification of the linear (6):

$$\sqrt{2}(\partial_\tau + i\delta_n)y_n^{\pm} = \;\; e^{\mp i\theta}\alpha_n^{-}y_{n-1}^{\pm} + e^{\pm i\theta}\beta_n^{-}y_{n-1}^{\mp}$$
$$+\, e^{\pm i\theta}\alpha_n^{+}y_{n+1}^{\pm} + e^{\mp i\theta}\beta_n^{+}y_{n+1}^{\mp}, \qquad (19)$$

where $\delta_n^{\pm} \doteq \Lambda r(r^2 + n^2)$, $\Lambda \doteq \lambda/\mathcal{A}p^3$, and $\alpha_n^{\pm}$, $\beta_n^{\pm}$ are as in (6). In the large-$|n|$ limit, one has $\alpha_n^{\pm} \sim 1$, $\beta_n^{\pm} \to 0$, $\delta_n \sim \Lambda n^2$, so one obtains the following scaling: $|y_{n+1}^{\pm}| \sim |y_n^{\pm}|/\Lambda n^2$.

This shows that the harmonic magnitude $|y_n|$ decreases rapidly (super-exponentially) with $|n|$, and thus low-order truncations may be justified. Note that although the opposite scaling, $|y_{n-1}^{\pm}| \sim |y_n^{\pm}|/\Lambda n^2$ is also formally possible, such modes cannot be excited, as is the case with inward propagating PSWs. Figure 6(a) shows that, indeed, the agreement between analytical QL growth rates and nonlinear DNS improves as the parameter Λ increases. The agreement becomes nearly perfect for $\Lambda \gtrsim 0.5$. Figure 6(b) shows that the same effect can be achieved if, instead of the λ term in (18), one introduces sufficiently strong viscosity. In this case, one also has a modified (6) with the exact form of (19), but with $\delta_n^{\pm} \doteq \mu(r^2 + n^2)$, where $\mu \doteq \nu_+/\mathcal{A}p^2$ (with $\nu_- = 0$ for simplicity). Again, the agreement becomes nearly exact for $\mu \gtrsim 0.5$.

SUMMARY

In this paper, we explore structure formation in two-dimensional MHD turbulence as a modulational instability (MI) of turbulent fluctuations. We focus on the early stages of structure formation and consider simple backgrounds that allow for a tractable model of the MI while retaining the full chain of modulational harmonics. This approach allows for a systematic examination of the importance of high-order correlations that are typically ignored in mean-field theories.

We find that, when the primary structure truly experiences a MI, this MI can be described well with the QLA which neglects high-order correlations. However, in adjacent regimes, such truncated models can fail spectacularly and produce false
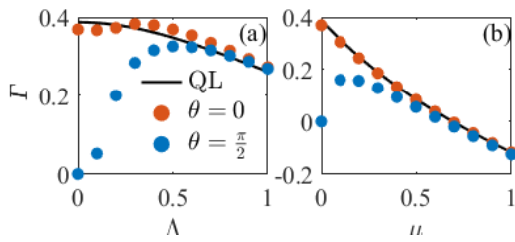
Figure 6. The growth rate Γ, at $\nu_- = 0$, versus: (a) $\Lambda \doteq \lambda/\mathcal{A}p^3$ and (b) $\mu \doteq \nu_+/\mathcal{A}p^2$. The colour markers indicate the results obtained through DNS of (6), while the black solid curves indicate solutions obtained from the QL truncation of (19). The results are presented for the representative cases $\theta = 0$ and $\theta = \pi/2$, both at $r = 0.5$.

positives for instability. To study this process in detail, we propose an 'extended' quasilinear theory (XQL) that treats the primary structure as fixed but includes the entire spectrum of modulational harmonics (as opposed to just the low-order harmonics, as usual). We find that the difference between said regimes is due to a fundamental difference in the structures of the modulational spectra. For unstable modes, the spectrum is localized at low harmonic numbers, so truncated models are justified. But this localization does not always occur.

At other parameters, modulational modes turn into constant-amplitude waves propagating down the spectrum, unimpeded until dissipative scales. These spectral waves are self-maintained as global modes with real frequencies and cause ballistic energy transport along the spectrum, breaking the feedback loops that could otherwise sustain MI.

The ballistic transport by PSWs drains energy from the primary structure at a constant rate until the primary structure is depleted. Because global PSWs exist at almost all parameters, this means that almost any primary structure in ideal incompressible MHD will eventually be depleted. This means, in particular, that sustainability of MHD structures is not entirely limited to the issue of exponentially growing linear instabilities, as PSWs must also be taken into consideration.

Finally, we find that departures from ideal MHD constrains the form of modulational eigenmodes, in turn suppressing the amplitude of high harmonics. This allows us to end on an informed yet optimistic note regarding the applicability of the QLA for structure formation in dispersive forms of MHD. That said, it is an important conclusion of our work that, unless deviations from ideal incompressible MHD are substantial, changing the turbulence parameters even slightly can destroy the applicability of an otherwise workable reduced model. An understanding of the complex modulational dynamics supported by (nearly) incompressible MHD aids the interpretation of existing simple closures and potentially opens the path to building more reliable alternatives.

REFERENCES

Bender, C. M. 2005 Introduction to $\mathcal{PT}$-symmetric quantum theory. *Contemp. Phys.* **46**, 277.

Beresnyak, A. 2019 MHD turbulence. *Living Rev. Comput. Astrophys.* **5** (1), 2.

Biskamp, D. 2003 *Magnetohydrodynamic Turbulence*. Cambridge Univ. Press.

Blackman, E. G. & Field, G. B. 2002 New dynamical mean-field dynamo theory and closure approach. *Phys. Rev. Lett.* **89**, 265007.

Brandenburg, A. 2018 Advances in mean-field dynamo theory and applications to astrophysical turbulence. *J. Plasma Phys.* **84** (4), 735840404.

Brandenburg, A., Sokoloff, D. & Subramanian, K. 2012 Current status of turbulent dynamo theory: from large-scale to small-scale dynamos. *Space Sci. Rev.* **169**, 123–157.

Dodin, I. Y. 2022 Quasilinear theory for inhomogeneous plasma. *J. Plasma Phys.* **88**, 905880407.

Donzis, D. A., Sreenivasan, K. R. & Yeung, P. K. 2005 Scalar dissipation rate and dissipative anomaly in isotropic turbulence. *J. Fluid Mech.* **532**, 199–216.

Gopalakrishnan, K. & Singh, N. K. 2023 Mean-field dynamo due to spatio-temporal fluctuations of the turbulent kinetic energy. *J. Fluid Mech.* **973**, A29.

Heinonen, R. A., Diamond, P. H., Katz, M. F. D. & Ronimo, G. E. 2023 Generation of momentum transport in weakly turbulent β-plane magnetohydrodynamics. *Phys. Rev. E* **107**, 025202.

Hussain, A. K. M. Fazle 1986 Coherent structures and turbulence. *J. Fluid Mech.* **173**, 303–356.

Jin, S. & Dodin, I. Y. 2024 On reduced modeling of the modulational dynamics in magnetohydrodynamics.

Käpylä, P. J., Korpi, M. J., Ossendrijver, M. & Stix, M. 2006 Magnetoconvection and dynamo coefficients - III. α-effect and magnetic pumping in the rapid rotation regime. *Astron. Astrophys.* **455** (2), 401–412.

Kraichnan, R. H. 1977 Eulerian and Lagrangian renormalization in turbulence theory. *J. Fluid Mech.* **83** (2), 349–374.

Krashennikov, S. I., D'Ippolito, D. A. & Myra, J. R. 2008 Recent theoretical progress in understanding coherent structures in edge and SOL turbulence. *J. Plasma Phys.* **74** (5), 679–717.

Krause, F. & Rädler, K. H. 1980 *Mean-field Magnetohydrodynamics and Dynamo Theory*. Oxford: Pergamon Press.

Masada, Y. & Sano, T. 2014 Mean-field modeling of an α^2 dynamo coupled with direct numerical simulations of rigidly rotating convection. *Astrophys. J. Lett.* **794** (1), L6.

Moffatt, H. K. 1978 *Field Generation in Electrically Conducting Fluids*. Cambridge Univ. Press.

Nicklaus, B. & Stix, M. 1988 Corrections to first order smoothing in mean-field electrodynamics. *Geophys. Astrophys. Fluid Dyn.* **43** (2), 149–166.

Rädler, K. H. 1982 On dynamo action in the high-conductivity limit. *Geophys. Astrophys. Fluid Dyn.* **20** (3-4), 191–211.

Rädler, K. H. 2007 *Mean-Field Dynamo Theory: Early Ideas and Today's Problems*, pp. 55–72. Dordrecht: Springer Netherlands.

Rincon, F., Califano, F., Schekochihin, A. A. & Valentini, F. 2016 Turbulent dynamo in a collisionless plasma. *Proc. Natl. Acad. Sci. U.S.A.* **113** (15), 3950–3953.

Schekochihin, A. A. 2022 MHD turbulence: a biased review. *J. Plasma Phys.* **88** (5), 155880501.

Smolyakov, A. I., Diamond, P. H. & Malkov, M. 2000 Coherent structure phenomena in drift wave–zonal flow turbulence. *Phys. Rev. Lett.* **84**, 491–494.

Squire, J. & Bhattacharjee, A. 2015 Electromotive force due to magnetohydrodynamic fluctuations in sheared rotating turbulence. *Phys. Rev. E* **92**, 053101.

Tobias, S. M. 2021 The turbulent dynamo. *J. Fluid Mech.* **912**, P1.

Zakharov, V. E. & Ostrovsky, L. A. 2009 Modulation instability: The beginning. *Physica D* **238**, 540.

Zeldovich, Y. B. 1957 The magnetic field in the two-dimensional motion of a conducting turbulent fluid. *Sov. Phys. JETP* **4**, 460–462.